

KfK 3277
Januar 1982

Inclusive Break-up Reactions of ${}^6\text{Li}$ at an Incident Energy of 26 MeV / Nucleon

B. Neumann, H. Rebel, H. J. Gils, R. Planeta, J. Buschmann,
H. Klewe-Nebenius, S. Zagromski, R. Shyam, H. Machner

Institut für Angewandte Kernphysik
Institut für Radiochemie

Kernforschungszentrum Karlsruhe

KERNFORSCHUNGSZENTRUM KARLSRUHE

Institut für Angewandte Kernphysik
Institut für Radiochemie

KfK 3277

INCLUSIVE BREAK-UP REACTIONS OF
 ${}^6\text{Li}$ AT AN INCIDENT ENERGY OF 26 MeV/NUCLEON

B. Neumann, H. Rebel, H.J. Gils, R. Planeta,
J. Buschmann, H. Klewe-Nebenius, S. Zagromski,
R. Shyam⁺, and H. Machner⁺⁺

Kernforschungszentrum Karlsruhe GmbH, Karlsruhe

⁺ Science and Engineering Research Council, Daresbury Laboratory,
Daresbury, Warrington WA4 4AD, United Kingdom

⁺⁺ Kernforschungsanlage Jülich, Institut für Kernphysik

Als Manuskript vervielfältigt
Für diesen Bericht behalten wir uns alle Rechte vor

Kernforschungszentrum Karlsruhe GmbH
ISSN 0303-4003

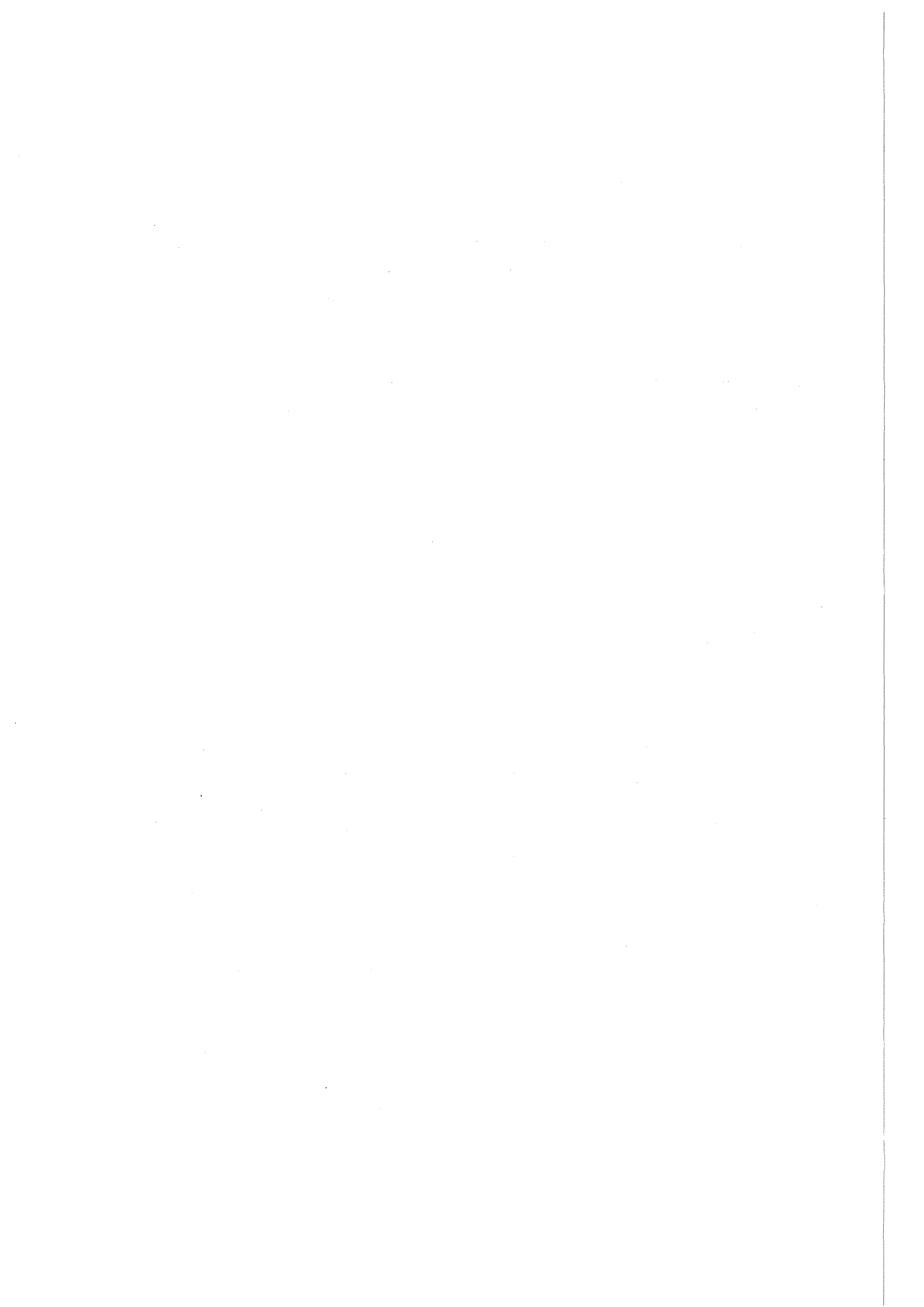
ABSTRACT

Inclusive charged particle spectra were measured from nuclear reactions induced by 156 MeV ${}^6\text{Li}$ on ${}^{40}\text{Ca}$. At forward angles the spectra exhibit broad break-up distributions centered around the energy corresponding to the beam velocity. The double differential cross sections together with previous results for a ${}^{208}\text{Pb}$ target were analyzed in the framework of the DWBA approach to projectile break-up taking into account elastic and inelastic reactions of the break-up fragments. The high energy tails of the background due to preequilibrium emission of complex charged particles were estimated on the basis of the coalescence model.

INKLUSIVE AUFBRUCHREAKTIONEN VON ${}^6\text{Li}$ BEI DER EINSCHUSS-
ENERGIE VON 26 MeV/NUKLEON

ZUSAMMENFASSUNG

Es wurden die inklusiven Energiespektren leichter geladener Teilchen beim Beschuß von ${}^{40}\text{Ca}$ mit 156 MeV ${}^6\text{Li}$ -Ionen gemessen. Bei Vorwärtsemissionswinkeln zeigen die Spektren breite Verteilungen von Aufbruchfragmenten, deren Energien um jene Energien zentriert sind, die der Strahlgeschwindigkeit entsprechen. Die gemessenen doppelt-differentiellen Wirkungsquerschnitte wurden zusammen mit früheren Resultaten für ${}^{208}\text{Pb}$ Targets im Rahmen einer DWBA-Aufbruchtheorie analysiert, wobei neben elastischen auch inelastische Prozesse berücksichtigt werden. Die hochenergetischen Ausläufer der Präequilibriumsemission komplexer geladener Teilchen, die den Untergrund unter den Aufbruchskomponenten darstellen, wurden auf der Basis des Koaleszenz-Modells abgeschätzt.



1. INTRODUCTION

Recently there has been considerable interest in studies of the emission of light charged particles in reactions between two complex nuclei ¹⁾. These processes are characterized by rather large cross sections and unusual shapes of the energy spectra. In addition to complete fusion which leads to formation of a compound nucleus, and to the emission of particles preceding the compound nucleus equilibration, the break-up of projectiles in the nuclear field has been found to be a dominant reaction channel accounting for a significant fraction of the total reaction cross section of light and heavy ion induced reactions ²⁻¹¹⁾, in particular at energies above 10 MeV/nucleon. Broad peaks centered near energies corresponding to the beam velocity signal the occurrence of projectile fragmentation. The inclusive spectra are basically interpreted to originate from fragments in a spectator role, reflecting the momentum distribution of the fragments in the projectile before the collision. Various simple models ^{4,6,12-16)} based on quasi free scattering mechanisms describe the shapes of the break-up cross sections fairly well. However, these models account only for the elastic break-up mode and neglect inelastic modes, in particular processes in which the unobserved fragment is transferred to the target. Such incomplete fusion processes (also known as "absorptive break-up", "massive transfer", "internal break-up", "stripping to the continuum") have been experimentally found to contribute predominantly to the inclusive spectra of the emitted particles ¹⁷⁻¹⁹⁾.

Recently several theoretical approaches ²⁰⁻²⁵⁾ have been worked out which provide more realistic descriptions of the experimental situation. The DWBA break-up theory as developed by Baur, and coworkers ²⁰⁻²²⁾ based on a one-step break-up mechanism ("spectator mechanism") enables calculations of the inelastic break-up contributions to the inclusive cross section. This particular theory has been proven to be quite successful in describing the break-up of deuterons, ³He, α -particles and ⁹Be (for a review see ref. 2) and certainly it is of interest to look into further cases.

There is also another simple mechanism which may contribute to the inclusive spectra: inelastic excitation of the projectile to continuum states and subsequent decay into fragments. Such a "sequential break-up mechanism" seems to be important for deuteron break-up reactions at low incident energies on high Z target nuclei²³⁾, and for heavy ions²⁴⁾. Tamura, Udagawa and coworkers²⁵⁾ have studied the break-up of heavy ions in the framework of a final state interaction model.

For studying the general features of break-up mechanisms of complex projectiles in the field of a nucleus, ${}^6\text{Li}$ is a very interesting and rather unique probe. On one hand ${}^6\text{Li}$ -induced nuclear reactions are accessible to a more microscopic understanding like reactions induced by lighter nuclear probes. On the other hand there are features which indicate the transition to a behaviour typical for heavy ions. The large probability of the weakly bound ${}^6\text{Li}$ ($E_B = 1.47$ MeV) for breaking-up into two different fragments and the well-developed cluster structure emphasize just the reaction paths like break-up and transfer. With increasing ${}^6\text{Li}$ energy the break-up in the nuclear field competes more and more with the Coulomb break-up, and the mechanism tends to an immediate fragmentation of the ${}^6\text{Li}$ nucleus into continuum states.

In this paper the role of break-up reactions for the understanding of charged particle spectra from ${}^6\text{Li}$ induced nuclear reactions is demonstrated. We present the results of systematic measurements of the inclusive double-differential cross sections for emission of light charged particles after bombarding ${}^{40}\text{Ca}$ by 156 MeV ${}^6\text{Li}$ ions. The bumps around the beam velocity energy dominating the continuum part of the spectra are analyzed in terms of the DWBA break-up theory as formulated by Baur, Shyam, Rösler and Trautmann²⁰⁻²²⁾. However, due to the background from the high energy tail of preequilibrium emission, the comparison of the break-up theory and experimental cross sections requires an estimate of the contributions from background processes. For this the coalescence model²⁶⁾ has been invoked.

2. EXPERIMENTS AND RESULTS

2.1 Experimental Procedures

In a series of experiments ${}^6\text{Li}$ ions accelerated to 156 MeV by the Karlsruhe Isochronous Cyclotron were used to bombard ${}^{40}\text{Ca}$ targets (thicknesses: 4.5 - 10 mg/cm²). The primary goal was to measure the forward angle energy spectra of light charged ejectiles ($Z \leq 2$, $A \leq 4$) over an energy range extending from somewhat above the evaporation peak up to the maximum energy. A semiconductor counter telescope was used consisting of a 0.3 mm thick ΔE surface barrier silicon detector and two high purity Ge detectors with thicknesses of 15 mm and 20 mm, respectively. Using an additional telescope with a 6 mm thick surface barrier silicon E detector additional energy spectra of ${}^3\text{He}$ and α particles, particularly at large angles were measured. The detector solid angles were about 50 μsr and the angular resolution about 0.3°. Details of the experimental procedures including electronics, data handling are described in refs. 17,27,28. It was rather important to achieve a well focussed (halo free) particle beam as the projectile break-up yield is concentrated at forward angles where beam impurity effects would be most pronounced. In order to minimize beam halo, the beam was monochromized by a 150° analyzing magnet. Using a blank target frame it was verified that there was essentially no background down to 8°. The contributions from target impurities, in particular from oxygen could be estimated by measuring the elastic scattering at large angles and by the mass dependence of the break-up cross sections (see ref. 7).

2.2 Charged Particle Spectra

Differential energy spectra of outgoing protons, deuterons, tritons, ${}^3\text{He}$ and α particles were measured over an angular range from 9° to about 50°, in some cases up to 90°. Typical spectra are displayed in Figs. 1-3.

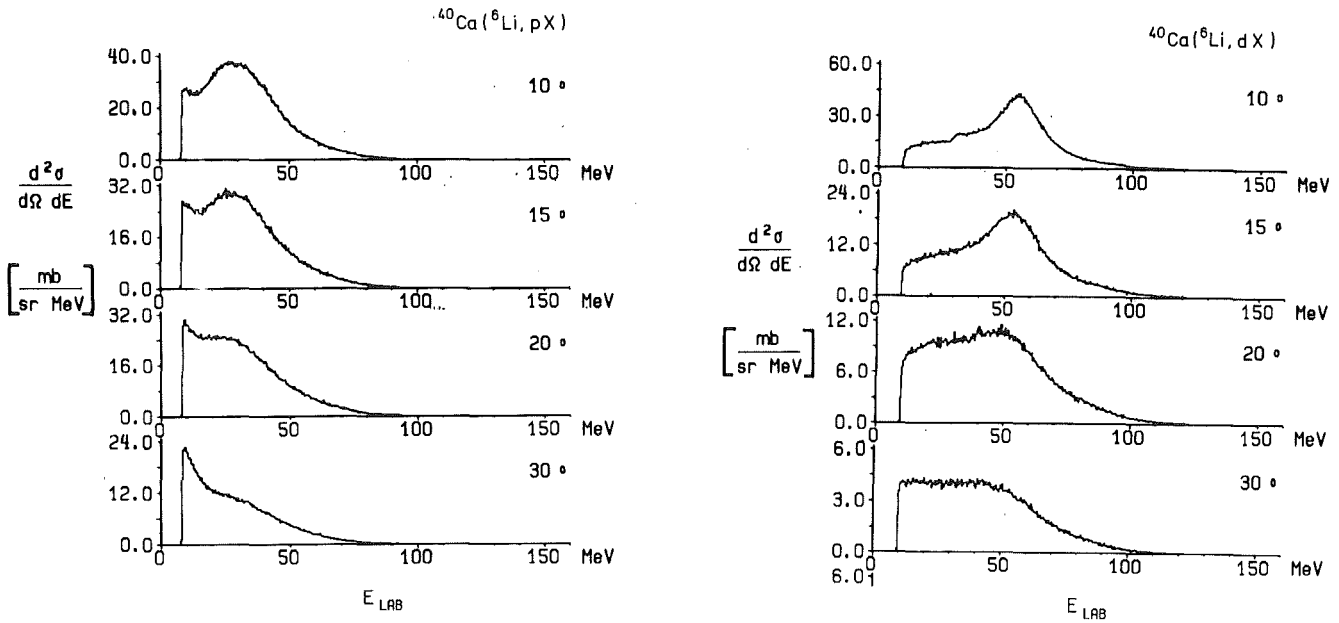


Fig. 1 Inclusive energy spectra of protons and deuterons from bombarding ^{40}Ca by $156\text{ MeV } ^6\text{Li}$ ions.

A more complete compilation of the measured double differential cross sections is given elsewhere ²⁹⁾. The thresholds at the low-energy ends of the spectra are due to the finite thickness of the ΔE -detector. The most striking features of the spectra can be summarized as follows:

- (1) As with other targets ^{7,17)} broad bumps are seen in each spectrum prevailing at forward angles. They are centered at energies corresponding approximately to the beam velocity, i.e., peaked at $E_x \cong m_x/m_{\text{Li}} \cdot E_{\text{Li}}$, where E_x , E_{Li} , m_x and m_{Li} are laboratory energies and masses of the observed ejectiles x and the incident ^6Li particle. The location of the peaks is slightly shifted towards lower energies with increasing angles.

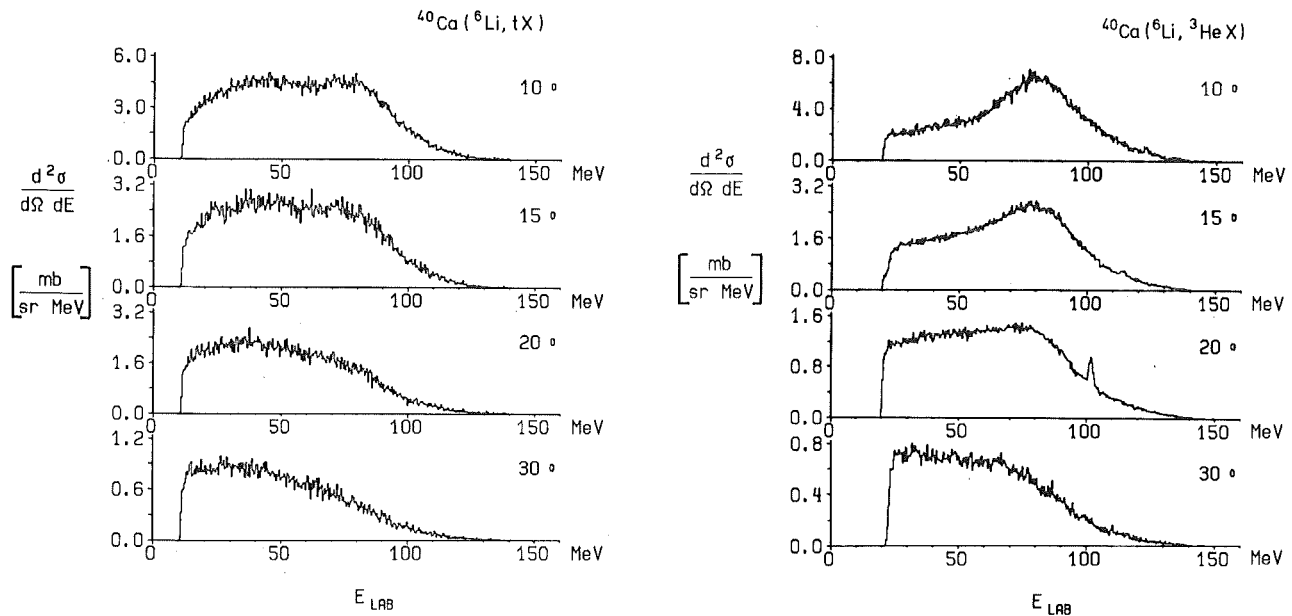


Fig. 2 Inclusive energy spectra of tritons and ${}^3\text{He}$ from bombarding ${}^{40}\text{Ca}$ by $156\text{ MeV } {}^6\text{Li}$ ions⁺⁾

- (2) The yields vary rapidly with emission angle and fit into the systematics and the dependence on mass number A of the target as established by former studies⁷⁾.
- (3) In all spectra an underlying continuum due to preequilibrium emission is observed which extends to large angles. This background appears to be considerably more pronounced for ${}^{40}\text{Ca}$ than for heavier target

⁺⁾ The peak on the high energy tail of the ${}^3\text{He}$ spectra, rapidly varying in position with increasing angles, is not explained.

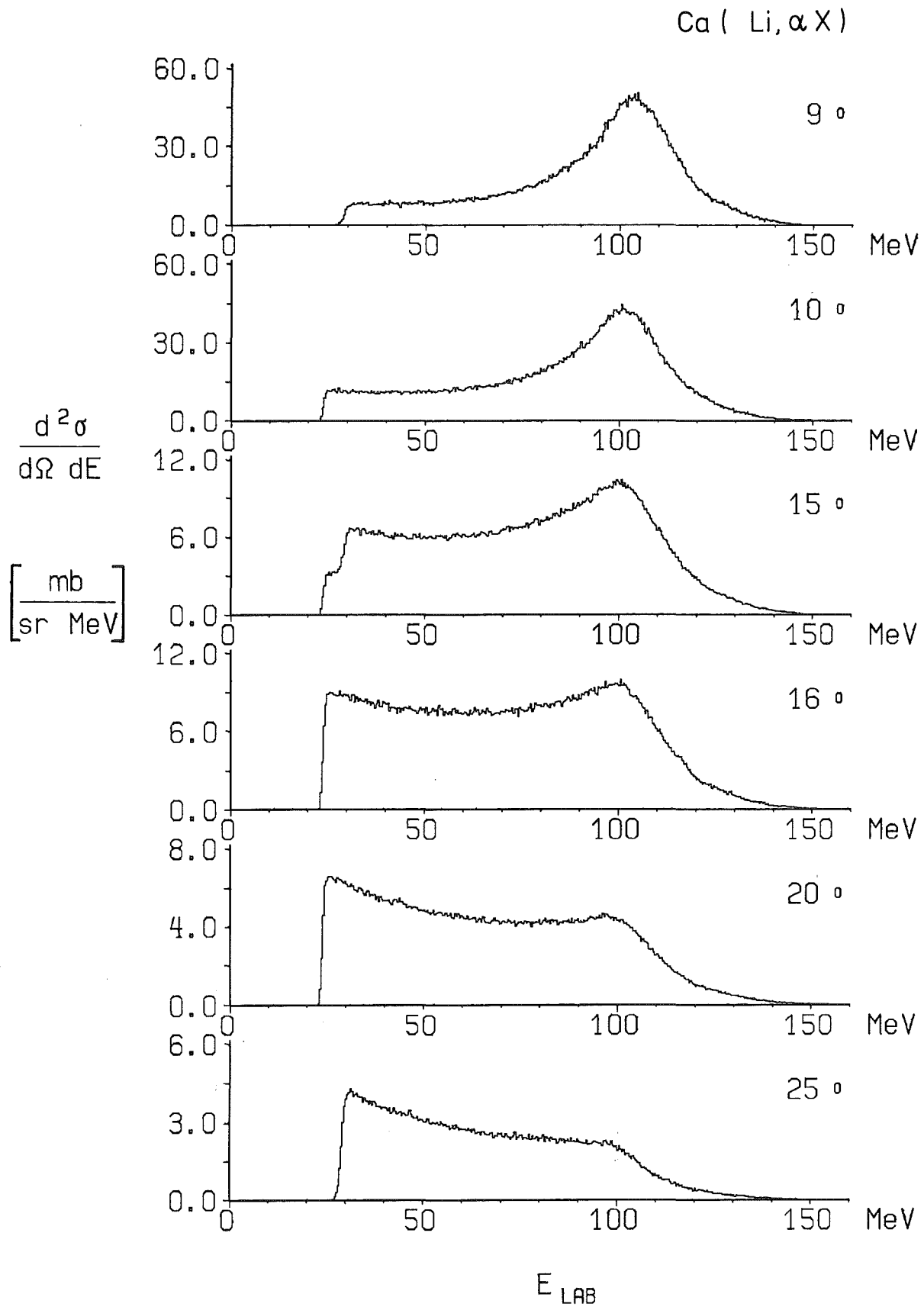


Fig. 3 Experimental α particle spectra for 156 MeV ${}^6\text{Li}$ incident on ${}^{40}\text{Ca}$ at various emission angles.

nuclei and causes difficulties when isolating the break-up contributions. In the proton spectra additional background arises from the tails of the proton evaporation yields.

In order to estimate total and differential cross sections in a consistent manner, we approximated the high energy tails from preequilibrium processes linearly and used the high energy halves of the break up bumps in evaluating the differential cross sections. The angular distributions appear to be exponentially decreasing by $d\sigma/d\Omega = Ce^{-\alpha\theta}$. Since the experimental angular distributions are not measured for extreme forward angles, the integrated break up cross sections σ_B are somewhat affected by the extrapolation of $d\sigma/d\theta$ to small angles ($<9^\circ$). However, it is known that the exponential shape of the angular distributions holds to angles quite smaller than the grazing angle^{30,17)} so that the overestimation by integrating to $\theta = 0^\circ$ does most likely not exceed 15%. Table 1 compiles extracted values*. A total reaction cross section value $\sigma_R = 1.981b$ results from optical model studies of 156 MeV ${}^6\text{Li}$ elastic scattering from ${}^{40}\text{Ca}$ ³¹⁾.

Table 1 Integrated break-up cross section σ_B and total break-up cross section σ_T for charged ejectiles

Particle observed	σ_B [b]	σ_B/σ_R	σ_T [b]	σ_T/σ_R	Target Energy
p	0.32	0.16			${}^{40}\text{Ca}$
d	0.36	0.18			
t^+	(0.28)	(0.14)			156 MeV
${}^3\text{He}$	0.08	0.04	1.48*	0.74	
α	0.44	0.22			

⁺ without background correction

*There might be an overcounting by simply adding the cross sections for particles of possibly binary fragmentation events.

(4) Compared to the α particle and deuteron cross sections the ^3He - and triton yields are much weaker. Unexpected shapes of the triton energy spectra being more complex than the ^3He spectra are found. In addition to the break-up triton component we recognize a further rather broad component, at lower energies, also observed with other targets^{7,17)}. Additional measurements have established that the shape of the triton component is not the result of particle identification problems, slit edge scattering or beam contaminants. By comparing the background in the triton and ^3He spectra at large angles (Fig. 4) we deduce that the "anomalous" low energy triton component decreases as rapidly as the other component.

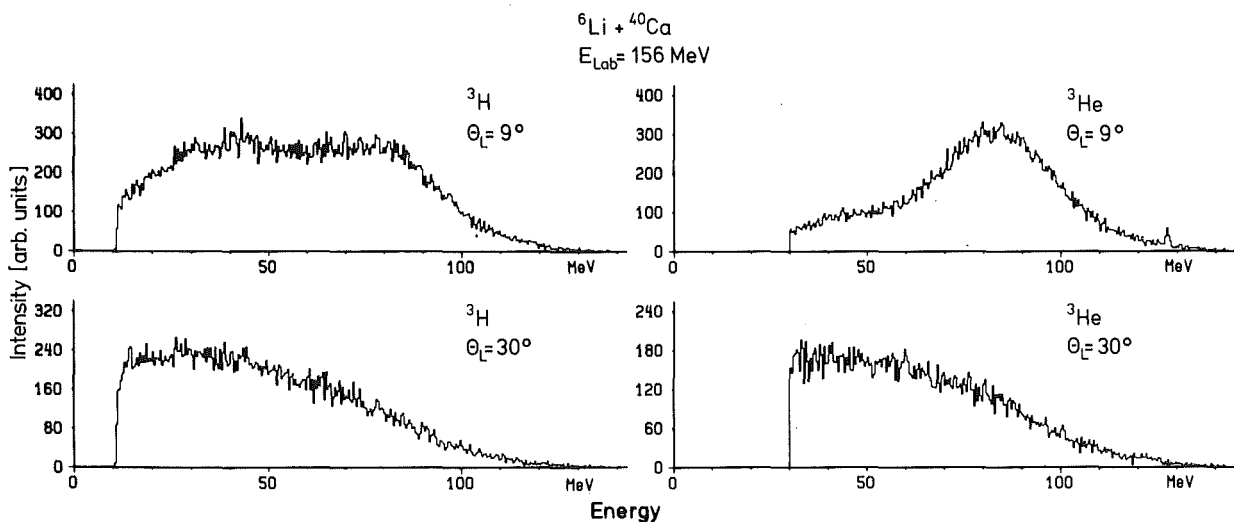


Fig. 4 Comparison of triton and ^3He spectra from bombardment of ^{40}Ca with 156 MeV ^6Li

The features of the broad bumps seen in all forward angle spectra are obviously consistent with peripheral fragmentation of the projectile in which the cross sections are primarily determined by properties of the projectile.

3. BREAK-UP THEORY

One of the most interesting aspects of projectile break-up reactions is the question to which extent the observed energy distributions of the fragments reflect their momentum distributions in projectile before break-up. The simplest picture of the break-up process is to assume that the interaction with the target nucleus simply cuts the projectile leaving the fragments with the same forward and internal momenta. The energy spectrum of each break-up fragment is thus peaked at an energy corresponding to the beam velocity when corrected for Coulomb effects. The bell-shaped distributions around the beam velocity reflect the internal Fermi momentum distribution. This is just the physical idea of plane wave break-up models like the early Serber model¹²⁾ where the break-up cross sections are essentially determined by the square $|\phi(\vec{p})|^2$ of the Fourier transform of the relative wave function of the constituents (i.e. the probability that the fragment has a momentum \vec{p} in the projectile) and by the available phase space. In fact, on this basis break-up reactions of light^{4,6,7,14,18)} and heavy particles^{9,15,16)} have been considered using several refinements and extensions of the quasi-free formulation of the theory and the models have been proven to be surprisingly successful. In the case of ${}^6\text{Li}$ break-up, e.g., the momentum distributions have been found⁷⁾ to be in agreement with results of quasi-elastic knock-out reactions of the type ${}^6\text{Li}(p,p\alpha)$ and ${}^6\text{Li}(\alpha,2\alpha)$. A more realistic description of the break-up process, however, requires the inclusion of inelastic processes such as target excitation and the absorption of the unobserved particle, in addition to a correct treatment of the distortion of incoming and outgoing waves. Such an approach has been developed by Baur, Shyam, Rösler and Trautmann²⁰⁻²²⁾. Before applying this theory (DWBABT) to the experimental data we review briefly the main ingredients (see e.g. Ref. 20 for details).

Using the post interaction form the cross section for the elastic break-up reaction $a+A \rightarrow b + x + A$ is written as

$$\frac{d^2\sigma(e1.)}{d\Omega_b dE_b} = 2\pi \frac{\mu_a \mu_b \mu_x}{(2\pi\hbar)^6} \frac{q_b q_x}{q_a} \frac{1}{(2j_a+1)} \int d\Omega_x \sum_{\mu_a \mu_b \mu_x} T_{\mu_a \mu_b \mu_x}(\vec{q}_a; \vec{q}_b \vec{q}_x) \quad (3.1)$$

where

$$T_{\mu_a \mu_b \mu_x} = \sum_{\substack{\ell m \ell \\ j \mu}} i^\ell \hat{\ell} B_{\ell m \ell}(\vec{q}_a; \vec{q}_b \vec{q}_x) \langle j_b \mu_b j_\mu | j_a \mu_a \rangle \langle \ell m_\ell j_x \mu_x | j \mu \rangle \quad (3.2)$$

and

$$\hat{\ell} B_{\ell m \ell}(\vec{q}_a; \vec{q}_b \vec{q}_x) = \int d\vec{r}_{bx} \int d\vec{R}_a \chi^{(-)*}(\vec{q}_b, \vec{R}_b) \chi^{(-)*}(\vec{q}_x, \vec{R}_x) * V_{bx}(r_{bx}) u_\ell(r_{bx}) Y_{\ell m_\ell}(\hat{r}_{bx}) \chi^{(+)}(\vec{q}_a, \vec{R}_a) \quad (3.3)$$

with $\hat{\ell} = (2\ell+1)^{1/2}$

In eq. (3.1) μ_a , μ_b and μ_x represent the reduced masses of particles a, b and x, respectively, and the integration is taken over the angles of the unobserved particle x. The quantities \vec{q}_a , \vec{q}_b and \vec{q}_x are the momenta of particles a, b and x in the initial and final channels. The interaction between b and x in a is denoted by $V_{bx}(r_{bx})$, and $u_\ell(r_{bx})$ is the radial part of the internal wave function of particle a. The χ 's denote the scattering wave functions of a, b and x generated by appropriate optical potentials. The integration over the angles of the unobserved particle in eq. (3.1) can be easily performed by introducing the partial wave expansion for $\chi^{(-)}(\vec{q}_x, \vec{R}_x)$ and using the orthogonality property of the spherical harmonics.

To simplify the computation of the T-matrix (eq. (3.2)) we introduce the zero range approximation. The use of this approximation for the reaction being investigated in this paper is less justified. However, while realizing the importance of performing a full finite range calculation, we would like to remind the reader that in our continuum situation quite a lot of values

(up to 50 or 60) of transfer angular momenta are involved in eq. 3.3. We feel, therefore, that performing a full finite range calculation by the standard methods³²⁾ may not be feasible at the moment. Hence, in this paper we avoid this and rely on the zero range approximation, even though it may introduce some uncertainties in our calculations. With this approximation eq. (3.1) reduces to

$$\frac{d^2\sigma(\text{el.})}{d\Omega_b dE_b} = \frac{2}{\pi} \frac{1}{E_a E_b} \left(\frac{\mu_x}{h^2}\right) \frac{q_x q_b}{q_a} D_0^2 \sum_{l_x m_x} |\hat{T}_{l_x m_x}^x|^2 \quad (3.4)$$

where

$$\hat{T}_{l_x m_x}^x = \sum_{l_a l_b} i^{l_a - l_b - l_x} e^{i(\sigma_{l_a} + \sigma_{l_b} + \sigma_{l_x})} \hat{l}_b \hat{l}_x$$

$$* \langle l_b - m_x \ l_x \ m_x | l_a \ 0 \rangle \langle l_b \ 0 \ l_x \ 0 | l_a \ 0 \rangle Y_{l_b - m_x}(\hat{q}_b) \quad (3.5)$$

$$* R_{l_a l_b l_x}$$

where

$$R_{l_a l_b l_x} = \frac{1}{q_x} \int \frac{dR}{R} \chi_{l_a}(q_a R) \chi_{l_b}\left(q_b \frac{A}{A+x} R\right) \chi_{l_x}\left(\frac{A}{A+b} q_x R\right) \quad (3.6)$$

and σ_{l_i} is the Coulomb phase-shift for the i^{th} particle, and the D_0^i is the zero range normalization constant.

Within rather well fulfilled approximations the inelastic break-up cross section can be calculated with the matrix elements already needed for the elastic break-up as following (see Ref. 21 for details),

$$\frac{d^2\sigma(\text{inel.})}{d\Omega_b dE_b} = \frac{2}{\pi} \frac{1}{E_a E_b} \left(\frac{\mu_x}{h^2}\right) \frac{q_b q_x}{q_a} D_0^2 \sum_{l_x m_x} \frac{\sigma_{l_x}^{\text{reaction}}}{\sigma_{l_x}^{\text{elastic}}} |\hat{T}_{l_x m_x}^x - \hat{T}_{l_x m_x}^0|^2$$

where $\sigma_{l_x}^{\text{elastic}}$ and $\sigma_{l_x}^{\text{reaction}}$ are the total elastic and the

reaction cross section for the interaction of x with target A . The t -matrix $T_{\ell x m_x}^{A0}$ has a form similar to eq. (3.5) with the wave function $\chi_{\ell x}$ replaced by regular Coulomb function.

Several values for D_0 have been reported in the literature³³⁾ which were essentially obtained by fitting the experimental data for (${}^6\text{Li}, d$) or ($d, {}^6\text{Li}$) reactions leading to the bound states of the residual nuclei, by zero range DWBA calculations. In the present calculation for the break-up of ${}^6\text{Li}$ into deuteron and α particle we have used a value of $-69.9 \text{ MeV fm}^{3/2}$ for D_0 . This value has been obtained by the usual definition of D_0 (see eq. Ref. 34) as

$$D_0 = \lim_{p \rightarrow 0} [G(p)]$$

where $G(p)$ is the Fourier transform of the s -wave part of $V_{bx}(r_{bx}) u_{\ell} r_{bx}$. The $V_{bx}(r_{bx})$ was obtained by assuming a Woods-Saxon-Form for the potential between α and deuteron whose depth was adjusted to give the correct separation energy for ${}^6\text{Li} \rightarrow \alpha + d$. The radius and the diffuseness parameter were taken to be 0.97 fm and 0.65 fm , respectively. The D_0 value calculated with such a simple method comes out to be surprisingly close to the values reported by Plattner et al.³⁵⁾ which are obtained by using the complicated forward dispersion relations.

It is interesting to note³⁶⁾ that if plane waves are inserted into eq. (3.3) for the particles a and b the break-up matrix element can be expressed in terms of the momentum space wave function of the particle b inside the nucleus α , thus giving the Serber formula¹²⁾ for the break-up process. Quite recently it has been shown by Hüfner and Nemes³⁷⁾ using Glauber theory, how the momentum distribution of the fragment is related to the Fermi motion. The momentum spectrum of the fragment can be related to the single particle momentum distribution specifically over the nuclear surface rather than the whole nucleus because of absorption.

A quite general formulation of the inclusive break-up processes was recently given by Austern and Vincent³⁸⁾, where the inclusive cross section is expressed in closed form as a ground state expectation value of an optical model propagator for the unobserved system. Introducing a peripheral approximation, the results presented in this paper are recovered³⁸⁾.

4. COMPARISON OF THE DWBA BREAK-UP THEORY WITH EXPERIMENTS

The analysis within the framework of the DWBA break-up theory requires as prerequisites the optical potentials (given in Table 2) for the fragments considered here) and the zero-range normalization constant D_0 which characterizes the strength of the interaction V_{xy} between the two cluster fragments (zero momentum component of V_{xy} * cluster wave function). With this input the theory predicts several experimental quantities, in particular

- (1) magnitude and shape (energetic position and width of the break-up bump) of the break-up cross section, which even in zero range approximation still reflects somehow the internal momentum distribution but affected by the distortion (orbital dispersion) by the optical potentials
- (2) the angular distribution
- (3) the ratio of elastic and inelastic break-up processes

Actually the comparison with the experimental results is hampered by the underlying background from preequilibrium emission (which we consider to be a different process though, in principle, there is a relation to inelastic break-up processes). Obviously, a complete understanding of the data requires a description of both types of the processes on the same theoretical basis.

Fig. 5 compares DWBAPT calculations of the α particle component from the ${}^6\text{Li} + {}^{208}\text{Pb}$ reaction at 156 MeV with experimental

cross sections given in ref. 7. For heavy target nuclei the background appears to be of reduced importance (particularly for forward angles). In fact, using a value of $D_0 = -69.3 \text{ MeV fm}^{3/2}$ as derived from a ${}^6\text{Li}$ cluster structure calculation (see sect. 3), the inclusive break up component at $\theta_L = 12^\circ$ is fairly well reproduced. However, Fig. 5 indicates that the experimental break-up yields decrease more rapidly with increasing angle than predicted. This may be a consequence of the zero range approximation which constraints²⁰⁾ the form of the intrinsic momentum space wave function of ${}^6\text{Li}$ to a Lorentzian shape $\phi(p) = D_0 / (\gamma^2 + p^2)$ where $\gamma^2 = 2 m \epsilon / \hbar^2$ with ϵ as the separation energy of the α -particle in ${}^6\text{Li}$.

Table 2 Optical potentials (Saxon-Woods form) used in the analysis of break-up cross sections

	V_0 [MeV]	r_v [fm]	a_v [fm]	W_0 [MeV]	r_w [fm]	a_w [fm]	Ref.
<u>${}^{40}\text{Ca}$</u>							
d	78.7	1.15	0.815	9.76	1.71	0.757	39
α	126.0	1.221	0.829	18.8	1.666	0.588	40
${}^6\text{Li}$	182.1	1.135	0.943	31.3	1.687	0.844	31
${}^3\text{He}$	113.3	1.19	0.78	18.6	1.676	0.588	41
<u>${}^{208}\text{Pb}$</u>							
d	90.5	1.15	0.755	9.01	1.63	0.626	39
α	146.	1.222	0.83	17.6	1.565	0.83	42
${}^6\text{Li}$	240.	1.17	0.766	20.0	1.554	1.015	31
${}^3\text{He}$	115.0	1.82	0.857	17.2	1.551	0.769	43

In the limit of a quasi free mechanism the angular distribution of the peak cross section, e.g., (corresponding to the minimum value $p = \frac{m_\alpha}{m_{\text{Li}}} p_{\text{Li}} \sin \theta$ contributing at particular emission angle θ) reflects the momentum distribution as well as the shape of $do/dE d\theta$ ("energy sharing distribution") at a fixed

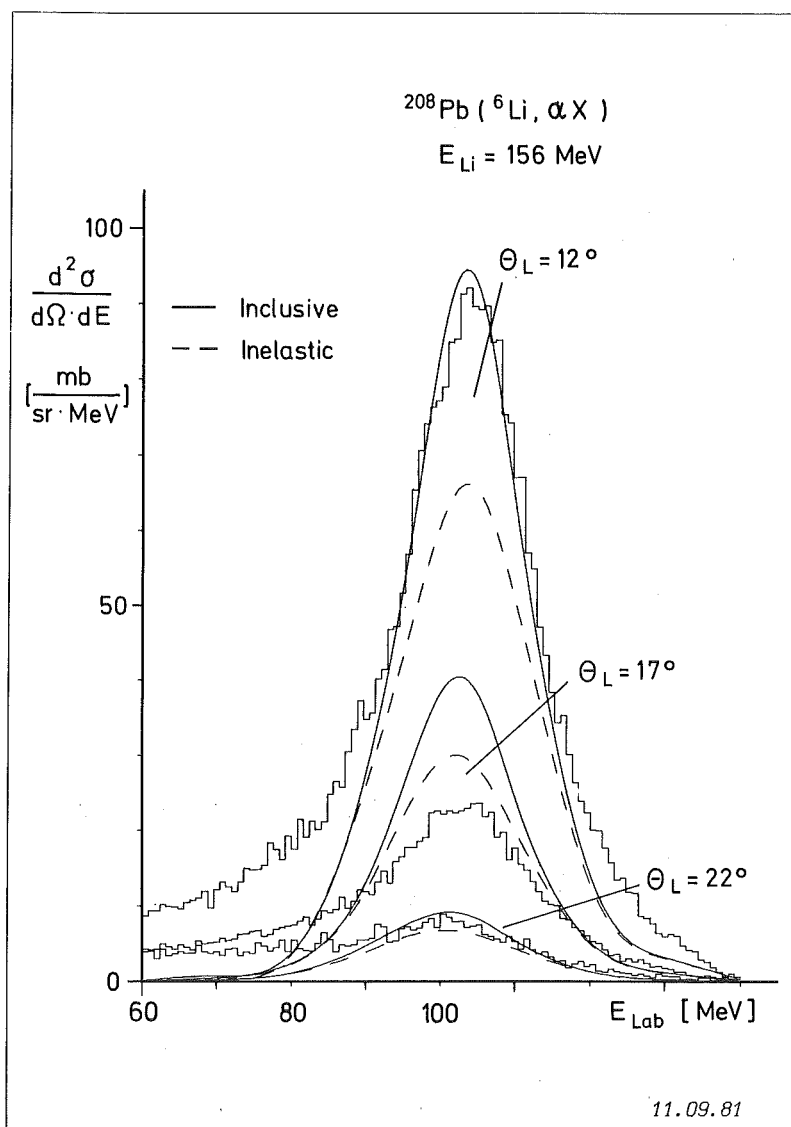


Fig. 5
 Experimental cross sections and theoretical predictions for break-up α particles from 156 MeV ${}^6\text{Li}$ on ${}^{208}\text{Pb}$

angle. To the extent to which the distortion does not disturb too seriously the spectator picture the observed defect of the zero range DWBA description indicates the sensitivity to the form of $|\phi(\vec{p})|^2$.

Further reasons for the incorrect theoretical description of the angular behaviour might be due to the use of optical potentials as derived from elastic scattering. The break-up itself has a strong effect on the elastic scattering

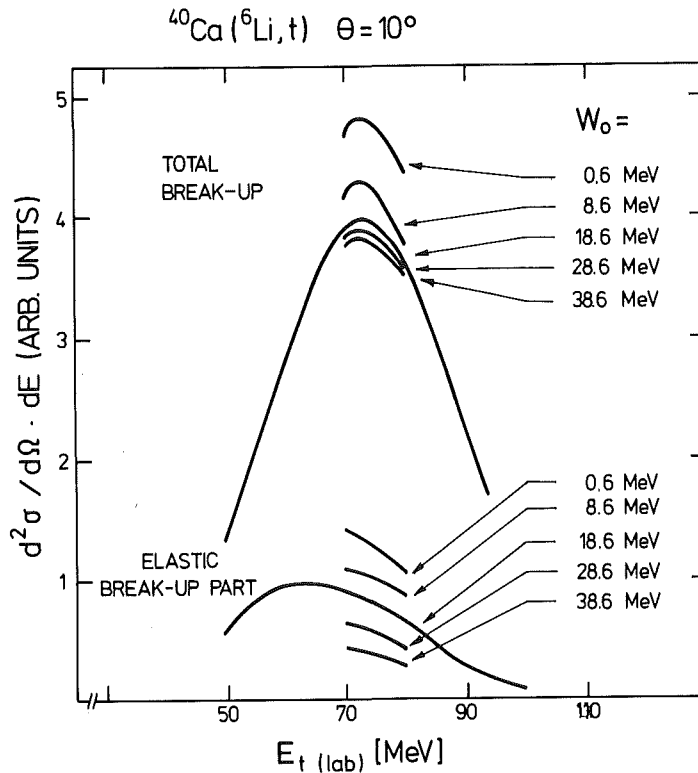


Fig. 6 The influence of the strength of the imaginary potential on the break-up cross section for the case $^{40}\text{Ca}({}^6\text{Li},t)$ calculated for 156 MeV ${}^6\text{Li}$ ions on the basis of the DWBA break-up theory.

cross section of the projectile and contributes strongly in particular to the absorptive part⁴⁴⁾ of the optical potential so that even the concept of DWBA becomes somewhat questionable. In Fig. 6 the influence of the imaginary strength is shown for the break-up of ${}^6\text{Li} \rightarrow t + {}^3\text{He}$ (where the optical potentials for ${}^3\text{He}$ and t are assumed to be identical, due to lack of better knowledge). The analysis of the ${}^3\text{He}$ and t spectra in terms of the DWBA break-up theory contains an additional uncertainty due to insufficient knowledge of the normalization constant. Anticipating that at forward emission angles the background in the ${}^3\text{He}$ spectra from bombarding ${}^{208}\text{Pb}$ is negligible, we fitted D_0 (${}^6\text{Li} = {}^3\text{He} + t$) at $\theta = 12^\circ$ and 17° and used the obtained value ($D_0 = -325 \text{ MeV fm}^{3/2}$) for the ${}^{40}\text{Ca}$ analysis.

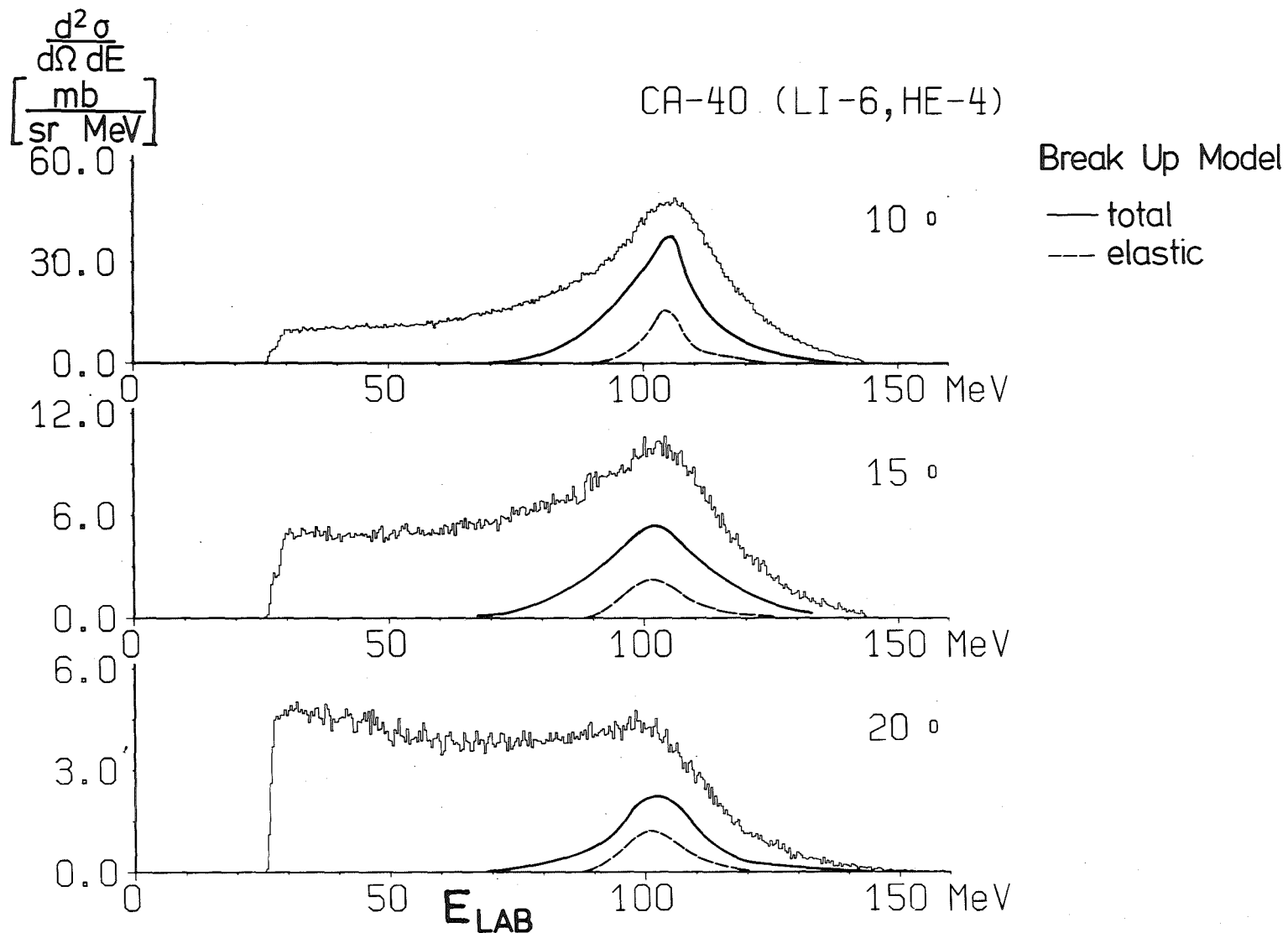


Fig. 7 Experimental cross sections for α -particle emission from the $^{40}\text{Ca}(^6\text{Li}, \alpha)$ reaction ($E_{\text{Li}} = 156 \text{ MeV}$) and theoretical predictions of the DWBA break-up model

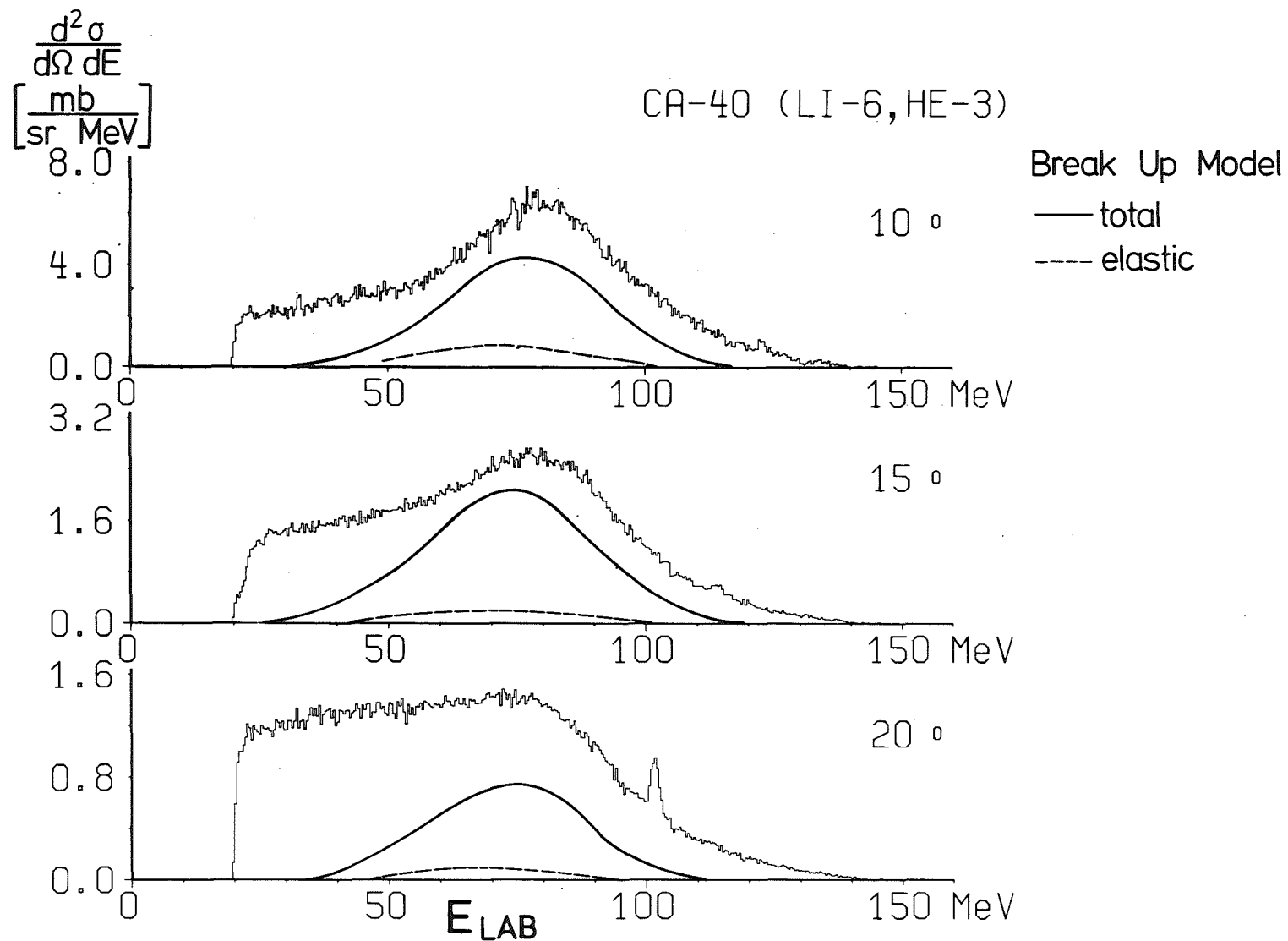


Fig. 8 Experimental cross sections for ${}^3\text{He}$ emission from the ${}^{40}\text{Ca}({}^6\text{Li}, {}^3\text{He})$ reaction ($E_{\text{Li}} = 156$ MeV) and theoretical predictions of the DWBA break-up model

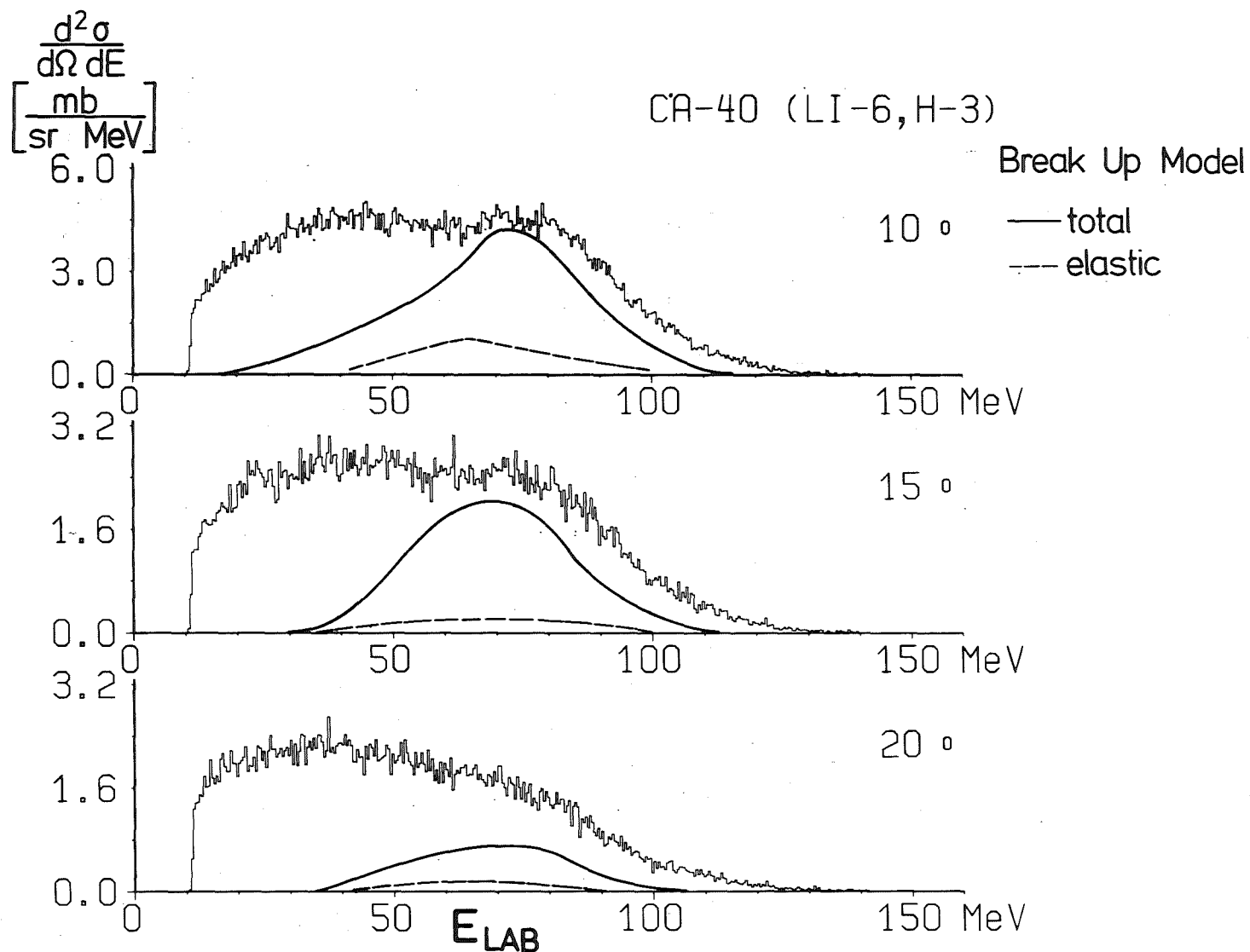


Fig. 9 Experimental cross sections for triton emission from the $^{40}\text{Ca}(^6\text{Li},t)$ reaction ($E_{Li} = 156$ MeV) and theoretical predictions of the DWBA break-up model

Figs. 7-9 display the results for the break-up reactions induced by the ^{40}Ca target and demonstrate the difficulties arising from the background and obscuring the comparison of theory and experiment. The theory predicts that the elastic break-up mode (where both fragments remain free) contributes only with a minor part. This feature has been experimentally demonstrated in previous studies¹⁷⁾. Small shifts between the maxima of the measured inclusive spectra and the predicted elastic part are significant and can be explained²⁾ by the difference in Q values for the elastic break-up and massive transfer (incomplete fusion) processes.

5. THE BACKGROUND FROM PREEQUILIBRIUM EMISSION

It has been shown²⁶⁾ that complex particle emission from p , d , ^3He and α particle induced reactions can be described within the exciton model by assuming the coalescence of excited nucleons to clusters. The only additional parameter entering into the calculation is the coalescence radius p_0 . The model basically assumes that nucleons with relative momenta less than p_0 condensate to a composite particle. Using the formulation of ref. 26 the cross sections are given by

$$\frac{d^2\sigma_x(E, \theta)}{dE d\Omega} = \sigma_0 \sum_{\substack{n=n_0 \\ \Delta n=2}} W_x(p, h, E, \theta) \tau_n$$

with σ_0 the total reaction cross section and τ_n the average n exciton life time. The angular distributions of the emission rates is determined by the angular distribution functions $A(p, h, \Omega_{p, h})$ which are the result of a recursion relation with the initial distribution function. More details of the procedures are found in ref. 26. When applying the model to the inclusive energy spectra and angular distributions of $p, d, t, ^3\text{He}$ and α particles emitted after bombarding ^{40}Ca by 156 MeV ^6Li ions the initial distribution function of the form

$$A(p_0, h_0, \Omega_{p_0, h_0}) = \pi^{-1} \cos\theta \theta (\pi/2 - \theta)$$

prove to be unable to reproduce the angular dependence of the spectra. Machner et al. ⁴⁵⁾ suggested an alternative form

$$A(p_0, h_0, \Omega_{p_0, h_0}) = A \exp(-a\theta)$$

introducing a further model parameter a in addition to the condensation probability γ_x which is related to the coalescence radius and the number of protons (π) and neutrons (ν) in the complex particle

$$\gamma_x = \gamma_{\pi+\nu} = \left[\frac{4}{3} \pi \left(\frac{p_0}{mc} \right)^3 \right]^{\pi + \nu - 1}$$

For the high excitation energy we have to deal with it is expected to be necessary to take into account a chain of particles emitted one after the other during the preequilibrium phase. For a particle of type y following the emission of a particle type x the cross section has been calculated as

$$\frac{d^2\sigma_{xy}(E_y, \theta)}{dE_y d\Omega_y} = \sigma_0 \sum_{\substack{n=n_0 \\ \Delta n=2}} \int dE_x W_x(p, h, E_x) \tau_n \sum_{\substack{m=m_0 \\ \Delta m=2}} W_y(p-p_x, h, E_y, \theta) \tau_m$$

with $m_0 = n - p_x$ and taking energy conservation into account. For practical calculations we have restricted ourselves for the first particle x to be only protons and neutrons. The total cross section for a given exit channel is then obtained by summation over all corresponding emission chains.

The parameters were adjusted by fitting the high energy tails of the measured spectra at $\theta_{\text{Lab}} = 45^\circ$ where the break-up components appear to be negligible. An optimum value $a=7 \text{ rad}^{-1}$ and values p_0 compiled in Table 3 are found.

Table 3 Used values of the coalescence radius

	t	³ He	α
p_0 [MeV/c]	271.	248	354

The values p_0 correspond to radii of the emitting volume roughly equal to the radii of the free clusters. It should be noted, however, that the parameters γ and p_0 , respectively, which provide the absolute scale of the preequilibrium emission spectra, are not very well determined by our procedure. Since even with including emission of a second particle the shapes of the spectra are not very well reproduced over the full energy range, fitting of high energy tails of the spectra at $\theta_{\text{Lab}} = 45^\circ$ is somewhat arbitrarily, and the resulting γ -values depend on which part is expected to be relevant for the fit. Therefore uncertainties in the order of 30 % must be accepted. Fig. 10-12 display the results when combining the coalescence model calculations with the DWBA break-up theory. The angular behaviour of first and second particle emission is different. The low energy evaporation parts are not shown as they do not extend to the region of beam-velocity particles. We reiterate that the not well determined values of γ affect the absolute values of the spectra. In the case of triton emission, e.g., a somewhat reduced value of γ would lead to better agreement. However, this would only varnish over the actual difficulties in understanding the continuum spectra. In addition to the uncertainties in the model parameters the discrepancies (obvious in Figs. 10-12) indicate that the coalescence model may account only for a fraction of the non-break-up contributions. Inelastic break-up processes may manifest themselves not only by the spectator particles but also in lower energy regions of the spectra via "higher order" processes like inelastic scattering of fragment particles, knock-out reactions⁴⁶⁾ etc.

6. CONCLUDING REMARKS

The interest in understanding the continuum spectra of charged particles emitted in ${}^6\text{Li}$ induced nuclear reactions has prompted to measure the inclusive cross sections and angular distributions of charged ejectiles in the case of bombarding

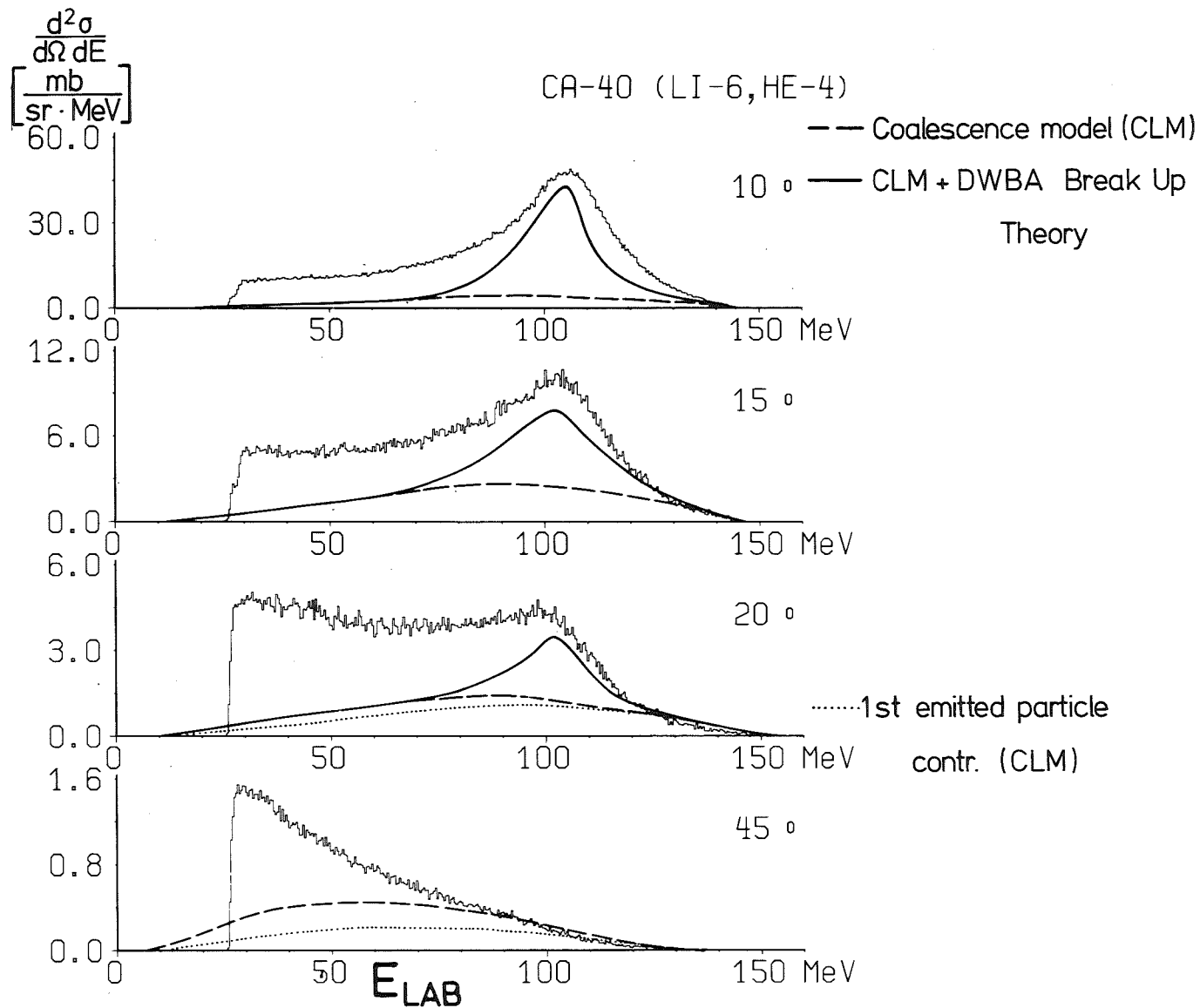


Fig. 10 $^{40}\text{Ca}(^6\text{Li}, \alpha x)$ at $E_{\text{Li}} = 156$ MeV: Preequilibrium emission background as predicted by the coalescence model

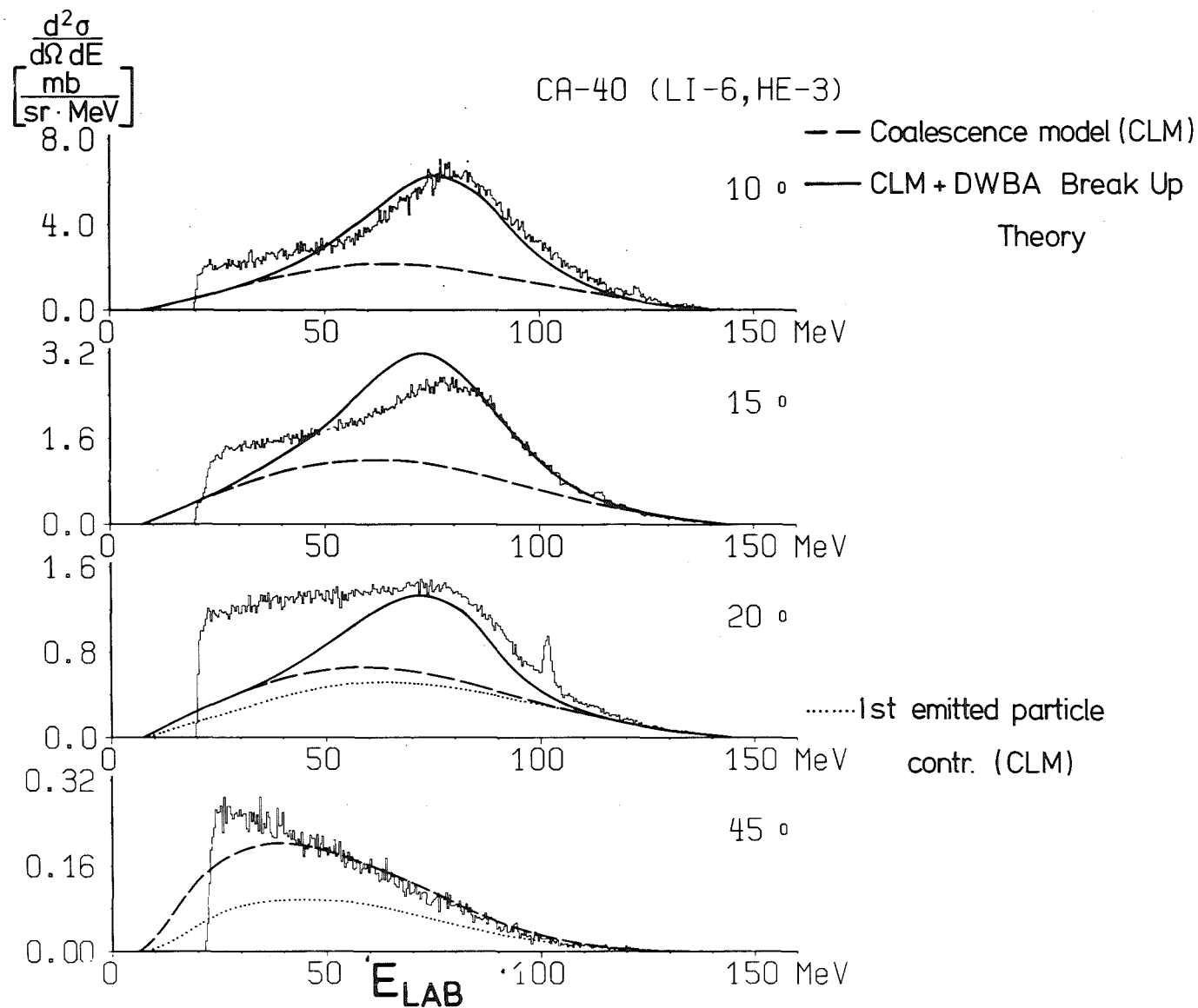


Fig. 11 $^{40}\text{Ca}(^6\text{Li}, ^3\text{He } x)$ at $E_{\text{Li}} = 156$ MeV: Preequilibrium emission background as predicted by the coalescence model

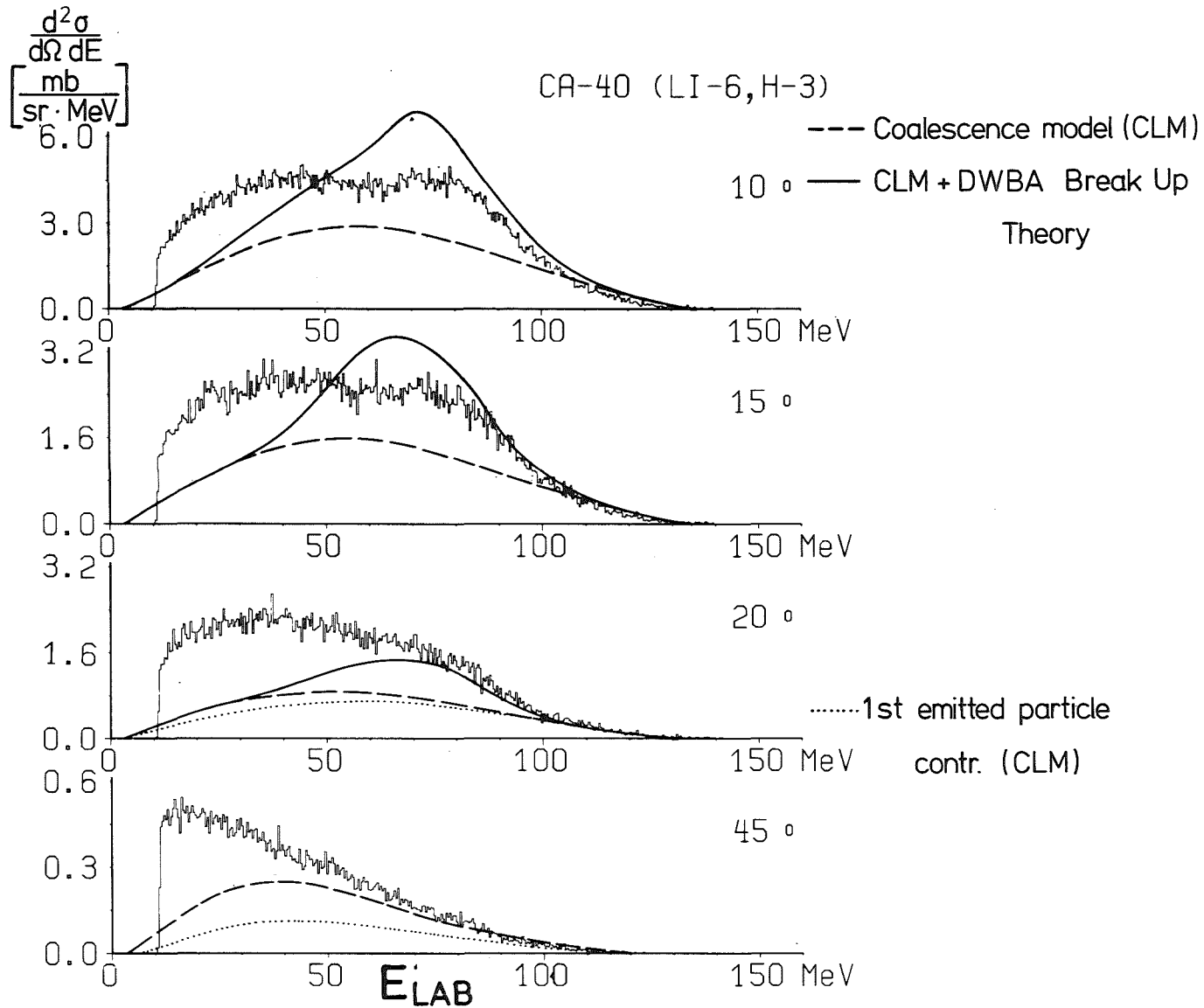


Fig. 12 $^{40}\text{Ca}(^6\text{Li}, tx)$ at $E_{\text{Li}} = 156$ MeV: Preequilibrium emission background as predicted by the coalescence model

^{40}Ca by 156 MeV ^6Li ions. Our studies were mainly focussed to the contribution of the projectile break-up signalled by broad distributions around the beam velocity energies in the spectra, dominating for the forward direction and rapidly decreasing with the emission angles. The general problem in analyzing the break-up part on the basis of the DWBA break-up theory arises from an unsufficiently understood background from different processes. The problem of interferences with other processes is particularly obvious in the case of triton emission where even the gross structure of the spectra cannot be fully explained. Tentatively, the exciton-coalescence model has been invoked in order to estimate the background from preequilibrium emission, but with modest success, partly due to insufficient knowledge of internal model parameters which determine the absolute scale and the angular behaviour of the preequilibrium emission cross sections. The background problem is reduced for the α -particle spectra where a more stringent test of the DWBA break-up theory seemed to be feasible. An important result of the comparison of theoretical predictions with experimental results is the failure in predicting the angular dependence of the cross sections correctly. This is most likely due to the simplification introduced by the zero range approximation implying a constraint for the internal momentum distribution of the fragment particles. Finite range calculations appear to be necessary to study such effects more in detail which would represent an interesting manifestation of the internal wave function of the projectile.

ACKNOWLEDGEMENT

We thank Professor Dr. G. Schatz and Professor Dr. R. Siemssen for their continuous interest and encouragement in this work and we acknowledge the efforts of the cyclotron operating crew in providing the ^6Li beam. We wish to express our gratitude to Dr. G. Baur, Dr. F. Rösler and Dr. D. Trautmann

for many useful discussions about the break-up theory and for supplying the DWBA computer code. One of the authors (R.S.) is also grateful to Dr. M.A. Nagarajan for many illuminating discussions, and to Professor Dr. G. Schatz for the kind hospitality of Kernforschungszentrum Karlsruhe extended to him during Winter of 1980.

REFERENCES

- 1) D.K. Scott: Proc. of 3rd Adriatic Europhysics Conference on Dynamics of Heavy Ion Collisions, HVAR, Yugoslavia, May 25-31, 1981.
- 2) A. Budzanowski: Proc. of 3rd Adriatic Europhysics Conference on Dynamics of Heavy Ion Collisions, HVAR, Yugoslavia, May 25-31, 1981.
- 3) J. Pampus, J. Bisplinghoff, J. Ernst, T. Mayer-Kuckuk, J. Rama Rao, G. Baur, F. Rösler, and D. Trautmann, Nucl. Phys. A311 (1978) 141.
- 4) J.R. Wu, C.C. Chang and H.D. Holmgren, Phys. Rev. C19 (1979) 370
U. Bechstedt, H. Machner, G. Baur, R. Shyam, C. Alderliesten, O. Bousshid, A. Djaloeis and P. Jahn, Nucl. Phys. A343 (1980) 221
J.R. Wu, C.C. Chang and H.D. Holmgren, Phys. Rev. Lett. 40(1978) 1013.
- 5) A. Budzanowski, G. Baur, C. Alderliesten, J. Bojowald, C. Mayer-Böricke, W. Oelert, P. Turek, F. Rösler, and D. Trautmann, Phys. Rev. Lett. 41 (1978) 635.
- 6) N. Matusoka, A. Shimizu, K. Hosono, T. Saito, M. Kondo, H. Sakaguchi, A. Goloa nd F. Oklani, Nucl. Phys. A 337 (1980) 269
- 7) B. Neumann, H. Rebel, J. Buschmann, H.J. Gils, H. Klewe-Nebenius, and S. Zagromski, Z. Phys. A 296 (1980) 113
- 8) C.M. Castaneda, H.A. Smith, Jr., P.P. Singh and H. Karwoski, Phys. Rev. C 21 (1980) 179
- 9) C.K. Gelbke, D.K. Scott, M. Bini, D.C. Hendrie, J.L. Laville, J. Mahoney, M.C. Mermaz and C. Olmer, Phys. Lett. 70B (1977) 425
- 10) H. Fröhlich, T. Shimodo, T. Ishihara, K. Nagatani, T. Udagowa, and T. Tamura, Phys. Rev. Lett. 42 (1979) 1518
- 11) Ch. Egelhaaf, G. Bohlen, H. Fuchs, A. Gamp, H. Homeyer and H. Kluge, Phys. Rev. Lett. 46 (1981) 813
- 12) R. Serber, Phys. Rev. 72 (1947) 1008

- 13) L. Landau and F. Lifshitz, JETP 18 (1948) 750
- 14) E.H.L. Aarts, P. Grasdijk, R.J. de Meijer and S.Y. van der Werf, Phys. Lett. 105B (1981) 130
- 15) M.S. Hussein and K.W. McVoy, in Continuum Spectra of Heavy Ion Reactions - Proc. of Int. Symp. Held in San Antonio, Texas, Dec. 3-5, 1979, ed. by T. Tamura, J.B. Natowitz and D.H. Youngblood, Harwood Academic Publishers.
- 16) S.L. Tabor, L.C. Dennis, K.W. Kemper, J.D. Fox, K. Abdo, G. Neuschaefer, D.G. Kovar, and H. Ernst, Phys. Rev. C24 (1981) 960
- 17) B. Neumann, J. Buschmann, H. Klewe-Nebenius, H. Rebel and H.J. Gils, Nucl. Phys. A339 (1979) 259
B. Neumann, H. Rebel, R. Planeta and R. Shyam, Proc. Europhys. Conf.: Nucl. and Atom. Phys. with Heavy Ions, 9-12 June 1981, Bucharest, Romania
- 18) R.W. Koontz, C.C. Chang, H.D. Holmgren, J.R. Wu, Phys. Rev. Lett. 43 (1979) 1862
- 19) H. Yamada, D.R. Zolnowski, S.F. Cola, A.C. Kohler, J. Pierce and T.T. Sugihara, Phys. Rev. Lett. 43 (1979) 605
- 20) G. Baur and D. Trautmann, Phys. Rev. 25C (1976) 293, G. Baur, F. Rösel and D. Trautmann, Nucl. Phys. A265 (1976) 101.
- 21) G. Baur, R. Shyam, F. Rösel and D. Trautmann, Helvetica Physica Acta, 53 (1980) 503
- 22) R. Shyam, B. Baur, F. Rösel and D. Trautmann, Phys. Rev. C22 (1980) 1401.
- 23) J. Kleinfeller, J. Bisplinghoff, J. Ernst, T. Mayer-Kuckuk, G. Baur, B. Hoffmann, R. Shyam, F. Rösel and D. Trautmann, Nucl. Phys. A370(1981) 150
- 24) J. von Driel, S. Gonggrijp, R.V.F. Janssens, R.H. Siemssen, K. Siwek-Wilczynska and J. Wilczynski, Phys. Rev. Lett. B98 (1981) 351
- 25) T. Udagawa, T. Tamura, T. Shimoda, H. Fröhlich, M. Ishihara and K. Nagatani, Phys. Rev. C20 (1979) 1949

- 26) H. Machner, Phys. Lett. 86B (1979) 129, Phys. Rev. C21 (1980) 2695
- 27) B. Neumann, KfK-Report 2887 (November 1979).
- 28) S. Zagromski, Int. Rep. Kernforschungszentrum Karlsruhe (unpublished).
J. Buschmann, Int. Rep. Kernforschungszentrum Karlsruhe (unpublished).
- 29) K. Feißt, B. Neumann, J. Buschmann, H.J. Gils and H. Rebel
Int. Rep. Kernforschungszentrum Karlsruhe (unpublished).
- 30) R.W. Ollerhead, C. Chasman and D.A. Bromley,
Phys. Rev. 134 (1969) B74
- 31) J. Cook, H.J. Gils, H. Rebel, H. Klewe-Nebenius
and Z. Majka, KfK-Report 3233 (1981).
- 32) N. Austern, Direct Nuclear Reaction Theories,
J. Wiley-Interscience, New York (1976).
- 33) H.W. Fullbright, Ann. Rev. Nucl. Part. Sci. 29 (1979) 161
- 34) A.A. Joannides, M.A. Nagarajan, and R. Shyam,
Nucl. Phys. A 363 (1981) 150
- 35) G.R. Plattner and R.D. Viollier, Nucl. Phys. A 365
(1981) 8
- 36) R. Shyam, G. Baur, F. Rösler and D. Trautmann,
Phys. Rev. C 19 (1979) 1246
- 37) J. Hüfner and M.C. Nemes, Phys. Rev. C23 (1981) 379
- 38) N. Austern and C.M. Vincent, Phys. Rev. C23 (1981) 1847
- 39) G. Mairle, K.T. Knöpfle, H. Riedesel, G.J. Wagner,
V. Bechtold, and L. Friedrich, Nucl. Phys. A339 (1980) 61
- 40) H.J. Gils, E. Friedman, H. Rebel, J. Buschmann,
S. Zagromski, H. Klewe-Nebenius, B. Neumann,
R. Pesl, and G. Bechtold, Phys. Rev. C21 (1980) 1239
- 41) T. Tanabe, M. Yasue, K. Wato, F. Soga, M. Igarashi,
K. Ogino, Y. Kadota, Y. Saito, S. Tanaka and F. Shimokoshi,
Nucl. Phys. A 311 (1978) 38
C. Gaarde, I.S. Larsen, A.G. Drentje, M.N. Harakeh,
S.Y. van der Werf, M. Igarashi, A. Müller-Arnke,
Nucl. Phys. A 346 (1980) 497

- 42) H.J. Gils, H. Rebel, J. Buschmann, H. Klewe-Nebenius, G.P. Nowicki, and W. Nowatzke, Z. Phys. A 219 (1976) 53
- 43) A. Djaloeis, J.-P. Didelez, A. Galonsky and W. Oelert, Nucl. Phys. A 306 (1978) 221
- 44) I.J. Thompson and M.A. Nagarajan, Phys. Lett. B106 (1981) 163
- 45) H. Machner, U. Bechstedt, A. Djaloeis, and P. Jahn, submitted for publication
- 46) W. Nitsche, G.J. Wagner, K.T. Knöpfle, P. Grabmayr, and H. Riedesel, Z. Physik A 300 (1981) 109